



Physical properties effect on photocatalytic degradation of phenol on TiO₂P25 thin films prepared by electrophoretic deposition

Akpène A. Dougna^{1,2}, Bertrand Gombert², Tomkouani Kodom¹,
Gbandi Djaneye-Boundjou¹, Sahidou O.B. Boukari², Limam M. Bawa¹

¹Laboratoire de Chimie des Eaux, Faculté des Sciences, Université de Lomé, BP : 1515, Lomé-Togo

²Institut de Chimie des Milieux et Matériaux de Poitiers, Université de Poitiers - CNRS, UMR 7285, TSA 41105 - 86073 Poitiers- France

Received 22 Sep 2017,
Revised 24 Nov 2017,
Accepted 30 Nov 2017

Keywords

- ✓ Electrophoretic deposition,
- ✓ diffusion,
- ✓ TiO₂P25,
- ✓ Phenol,
- ✓ Photocatalysis.

adougna@yahoo.fr ; Phone:
+22890964323;

Abstract

The preparation of thin layers of TiO₂P25 was implemented by electrophoretic deposition on conductive glass and stainless steel from a sol-gel suspension of TiO₂ during 40 s, 60 s, 80 s and 120 s. The mass of TiO₂ deposited on the substrate increases with the application time of the voltage. After deposition, the films obtained were first calcined in an oven at 450 °C for 1 hour and then used for photocatalytic degradation of phenol in aqueous solution at natural pH. Phenol removal kinetics was monitored using HPLC coupled with PDA detector and a phenyl column. The results revealed that in the case of the thin film prepared on steel, the photocatalyst amount seems to approach a plateau for high times of deposition. With regard to photocatalytic degradation, it appears that deposited mass does not influence the removal of phenol whatever the substrate. However, mineralization of phenol decreases with increasing of mass deposited on stainless steel but little change on conductive glass showing then the importance of physical properties of films on photocatalytic efficiency

1. Introduction

Photocatalysis is an advanced oxidation method widely studied in water treatment. This is a method to mineralize the refractory organic compounds from powerful radicals produced *in situ*. Several parameters can influence the kinetics and the mechanism of reaction carried out in aqueous media. These factors may be intrinsic to the catalytic material or related to the reaction medium [1-3]. One of the factors intrinsic to the material is the form of implementation of the catalyst. Indeed, the catalyst may be used in slurry form or as a deposit on an appropriate substrate. When the catalyst is used in suspension, a filtration step is necessary after degradation to extract the catalyst from the treated solution. For industrial pollution control applications, this leads to higher treatment costs despite undeniable process efficiency. In order to overcome this stage of separation of the aqueous medium treated catalyst, several techniques can be used to deposit the catalyst on a suitable support. Nevertheless, several authors agree on a reduction in the efficiency of photocatalysis [4] carried out with deposited catalysts. Similarly, methods of synthesis and preparation of catalysts have a strong influence on the photoactivity of the latter [5,6]. Several deposition methods like dip-coating [7,8], spin coating [7] or sputtering deposition [9] have been implemented from a colloidal solution of TiO₂ prepared by sol-gel method. Other methods like plasma sprayed induction [10], chemical vapor deposition (CVD) have also been used to make deposits of TiO₂ on the outer surface of the substrate [11,12], chemical vapor infiltration (CVI) to produce a film on the inner surface of the substrate and physical vapor deposition (PVD) [13,14]. There are also others methods derivative from latter, such as Low Pressure Chemical Vapor Deposition (LPCVD), Direct Liquid Injection Chemical Vapor Deposition (DLICVD), Metal Organic Chemical Vapor Deposition (MOCVD), Plasma Enhanced Chemical Vapor Deposition (PECVD) [15]. They differ from one another according to conditions of the reactions initiation and the implementation of the process. Each method has advantages and inconveniences related to cost, easiness of implementation, the proper control of the process (temperature, pH, reagents, solvents) and restriction due to the support [16].

One of the most interesting and widely used methods is electrophoretic deposition (EPD) [17-21]. Electrophoretic deposition is mainly done in two stages. Firstly, the charged particles migrate in an electric field toward the electrode having an opposite charge to theirs afterward the particles are deposited to form a dense layer. EPD is a useful technique because of morphology and thickness of the thin layers can be controlled by the applied voltage, deposition time and electrolyte concentration [18,21].

However, this technique leads to a reduction of the active surface available due to aggregate formation and reduction of pores of the catalyst material [4]. It is therefore necessary to have conditions to limit the cost of production while limiting the decrease in photoactivity of the deposited catalyst.

Previous works [22] reported that conducting glass is the best photocatalyst support for indigoid dye removal. It would be interesting to evaluate this support performance on other compound, like phenol, one refractory organic compound.

Fluorine doped Thin Oxide (FTO) is the most widely manufactured transparent conducting oxide (TCO) due to its thermal and chemical stability. In order to make transparent to visible light a semiconductor, it was necessary to have energy of band gap higher than 3.1 eV. At the same time, one reduces material conducting properties to visible light. TCOs are materials that have these two properties. In TCO with general formula (MxOy: D), oxide MxOy is doped in order to create, close to the conduction band, donor levels which allows the electrons moving from this level directly towards the conduction band. The quality of a TCO is related to the number of charge carriers and their mobility. TCO are used in several fields of activity such as photovoltaic cells, electrodes, deposit etc. A continuously use of renewable energies ensures a growth in demand for TCOs in future years [23]. Stainless steel can also be used as conductive substrates.

Therefore, the aim of the present work is to determine, according to physical properties studied, the best catalyst substrate between stainless steel and conducting glass FTO on the one hand, and on the other hand, the optimal amount of catalyst needed to obtain a good yield of phenol oxidation in our operating conditions.

2. Material and Methods

2.1. Material

All reagents were used without purification. Phenol (ACS grade) and methanol (HPLC grade) were purchased from Carlo Erba. The TiO₂ used was P25 from Evonik consisting of 80% anatase phase and 20% rutile phase (weight percentage) [24]. The solutions are prepared with ultrapure water produced by a Millipore system (TOC ≤ 0.2 mgC.L⁻¹; 18 MΩ.cm). Acetylacetone (≥ 99.5%) and the surfactant Triton X 100 are from Fischer Scientific. The substrates, conductive glass FTO (SnO₂: F, deposited thickness is about 80 nm, fluorine doped with CVD, Solems France) and stainless steel (304L) plates were used for deposits after carefully cleaning with a mixture of hydrogen peroxide and sulfuric acid. A UV-A lamp BLB (15 W electrical power) emitting primarily at 365 nm was used as a source of radiation in all photocatalytic experiments. The average intensity emitted by the lamp measured with the probe LP 471 UVA of a photoradiometer HD 2102.2 (DELTA OHM) is rated on average at 3.50 ± 0.5 W.m⁻². A scanning electron microscope (SEM) analysis were performed on a 7001 FEG type apparatus (JEOL) brand without special preparation or metallization. The layer thickness was assessed using the ImageJ software. Thin films of deposit were used for photocatalytic removal of phenol using the same flow loop irradiation reactor used for previous work (Fig.1) [25]. The detection and quantification of phenol were carried out with an HPLC (Waters Alliance 2695), coupled to a diode array detector (Waters 2998) using a Xbridge column of phenyl type (Waters, 150 x 4.6 mm, 5 μm). This system was used with a mobile phase consisting of water acidified with acetic acid (0.1%) (A) and methanol (B) using non-linear gradient mode (90% (A) to 100% (B)). Total organic carbon (mineralisation) was analysed by TOC-Vcsh (Shimadzu).

2.2. Preparation of thin films and photocatalytic degradation process

The preparation of thin films was made by electrophoretic deposition from a sol gel suspension in TiO₂ (P25) 12.5 g.L⁻¹. The preparation of the films was described previously (Fig. 1; [25]). A voltage of 10 V is applied between the two electrodes of the same remote area of 1 cm during several deposition times of 40 s, 60 s, 80 s and 120 s for the purpose of evaluating deposition time both on thickness and photocatalytic activity. The deposition surface is 125 ± 2 cm². After deposition, the plates are dried overnight at room temperature and then annealed at 450 °C in a muffle furnace for 1 h and used for photocatalysis of phenol solution (C₀ = 100 μmol.L⁻¹; V₀ = 900 mL). The choice of the annealing temperature is a key issue. It has been reported that at 450°C, no phase transition of TiO₂ occurs because of high activation energy needed. The crystal composition will remain unchanged at this temperature. Furthermore effect of prolonged calcination, more than 6 hours could be prejudicial for photocatalytic activity of deposit [24].

At the beginning of each experiment, two plates are placed in the irradiation reactor. After 1h of reaction in the dark, the phenol solution is irradiated for 180 min. It is generally accepted that in photocatalysis in dilute solutions ($C_0 < 10^{-3} \text{ mol.L}^{-1}$), the reaction kinetics follows the Langmuir-Hinshelwood model[26]. According to this model, the pollutant concentration at time t (min) is related to the apparent kinetic constant $k_{app}(\text{min}^{-1})$. This model has been applied in our study.

$$\ln(C/C_0) = -k_{app} \times t \quad \text{Equation 1}$$

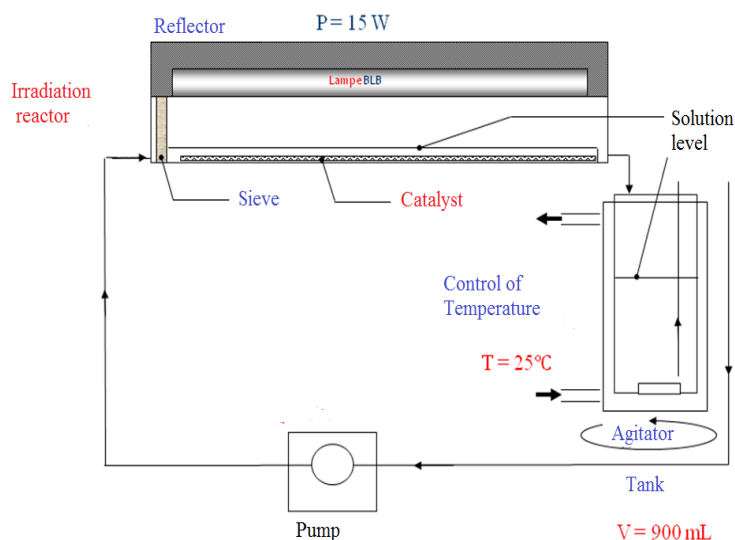


Figure 1. Photocatalytic reactor setup [25]

3. Results and discussion

3.1. Characterization of deposits by scanning electron microscopy

Deposits were analyzed by SEM to determine the relationship between the surface characteristic and thickness of the layers as a function of deposition time. The results of observation of thin films prepared on conducting glass for deposition times of 40 s (**Fig.2**) and 120 s (**Fig.3**) show a difference both in terms of the surface state and thickness. For the thin layer obtained with 40s of deposition time, the surface seems quite smooth with very few visible cracks in the selected viewing conditions. The measured thickness is about 3 μm . On the other hand, the surface of thin films prepared during 120 s present in the same observation conditions, significant cracking and high thickness of about 13 μm . The surface concentration and the tendency of deposits to crack therefore increase with deposition time. A similar observation was made by *Cui et al.*[20] after electrophoretic deposition of TiN on Ti substrates. The thickness of deposits increases quickly with time of deposition and changed after a certain settling time. They noted a thickness of 6.1 μm and 15 μm with the same electric field. The electrical force is the same as the applied voltage and the distance between the electrodes have remained unchanged. This phenomenon is due, according to these authors, to the decrease of the deposition current. What then could explain this decline in the deposit current?

Dor et al.[27] reported an almost similar observation in thicknesses ranging from 1.3 μm to 6.8 μm . This indicates that the cracking of the film surface would be relative to the nanoparticle aggregate type. Current decay and nanoparticle aggregate type would explain both surface morphology and difference between mass of deposit. Indeed Stokes law used to calculate sedimentation rate (**Equation 2**) gives the rubbing force F (N) influencing a charged particle in an electrical field:

$$F = 6\pi \times \eta \times r \times V \quad \text{Equation 2}$$

η : Dynamic viscosity (Pa.s)

r : Particle radius (m)

V : Velocity (m.s^{-1})

This force quickly balances the electric force qE . Therefore, according to a fundamental relationship in dynamics, particle velocity rapidly approaches a limit value v_1 [28] :

$$v_1 = \frac{q}{6\pi \times \eta \times r} E = \alpha E \quad \text{Equation 3}$$

α represents particle mobility and decreases with particle size (r).

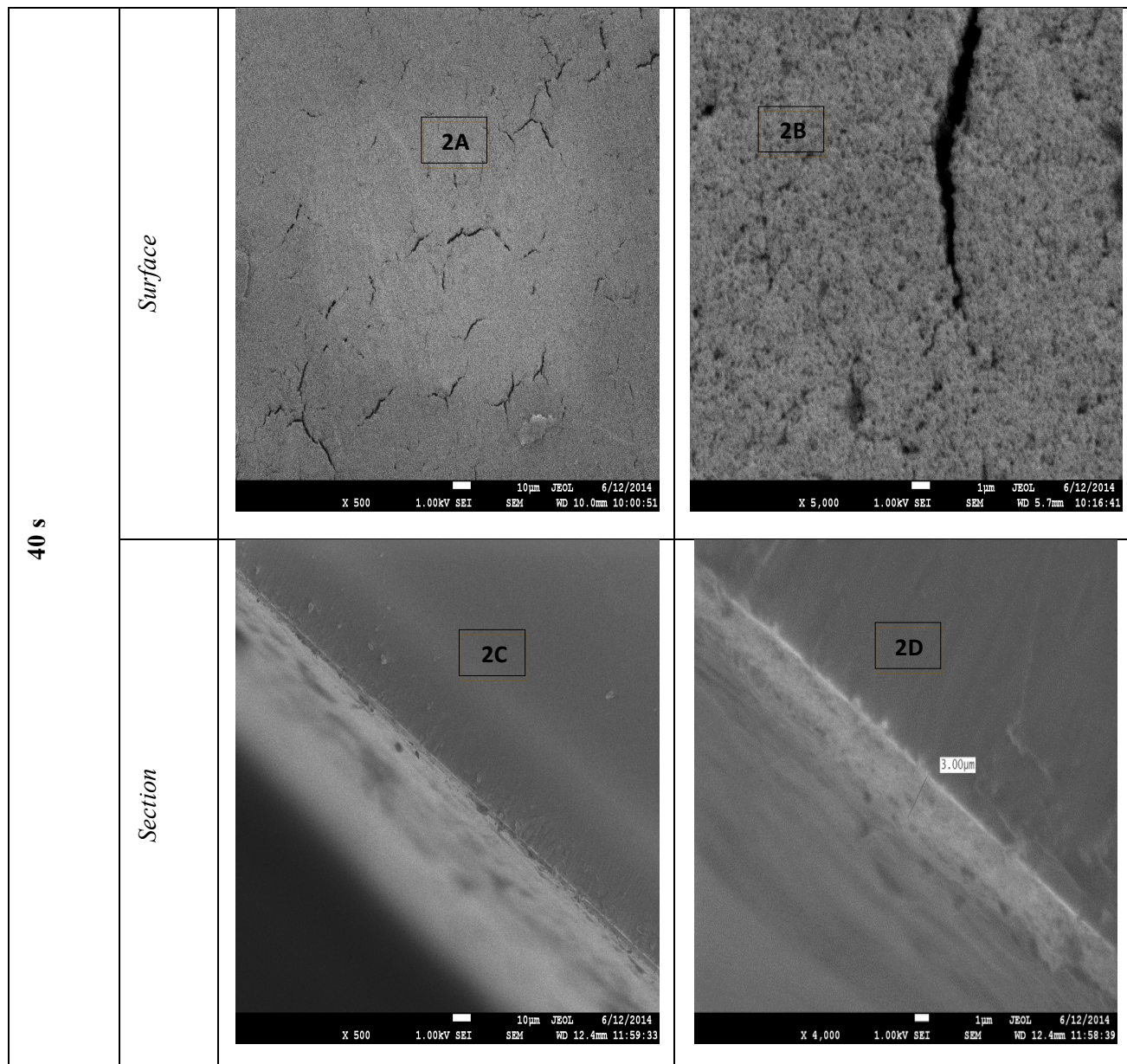


Figure 2. SEM image of thin film prepared on conducting glass during 40 s at different magnifications

Therefore the small aggregates formed during the electrophoretic deposition carried out during a relatively short time migrate more rapidly than large aggregates formed during the longer durations.

In addition, it is more difficult for large aggregates to form ordered structures. Furthermore sintering reduces distance between particles (**Fig.2B and Fig.3B**) and enhances the channels present in these structures due to internal stresses which appear as cracks (**Fig.2A and Fig.3A**). Consequently, the adhesion of thin layers prepared during 120 s will be less strong allowing particles detachment during photodegradation studies.

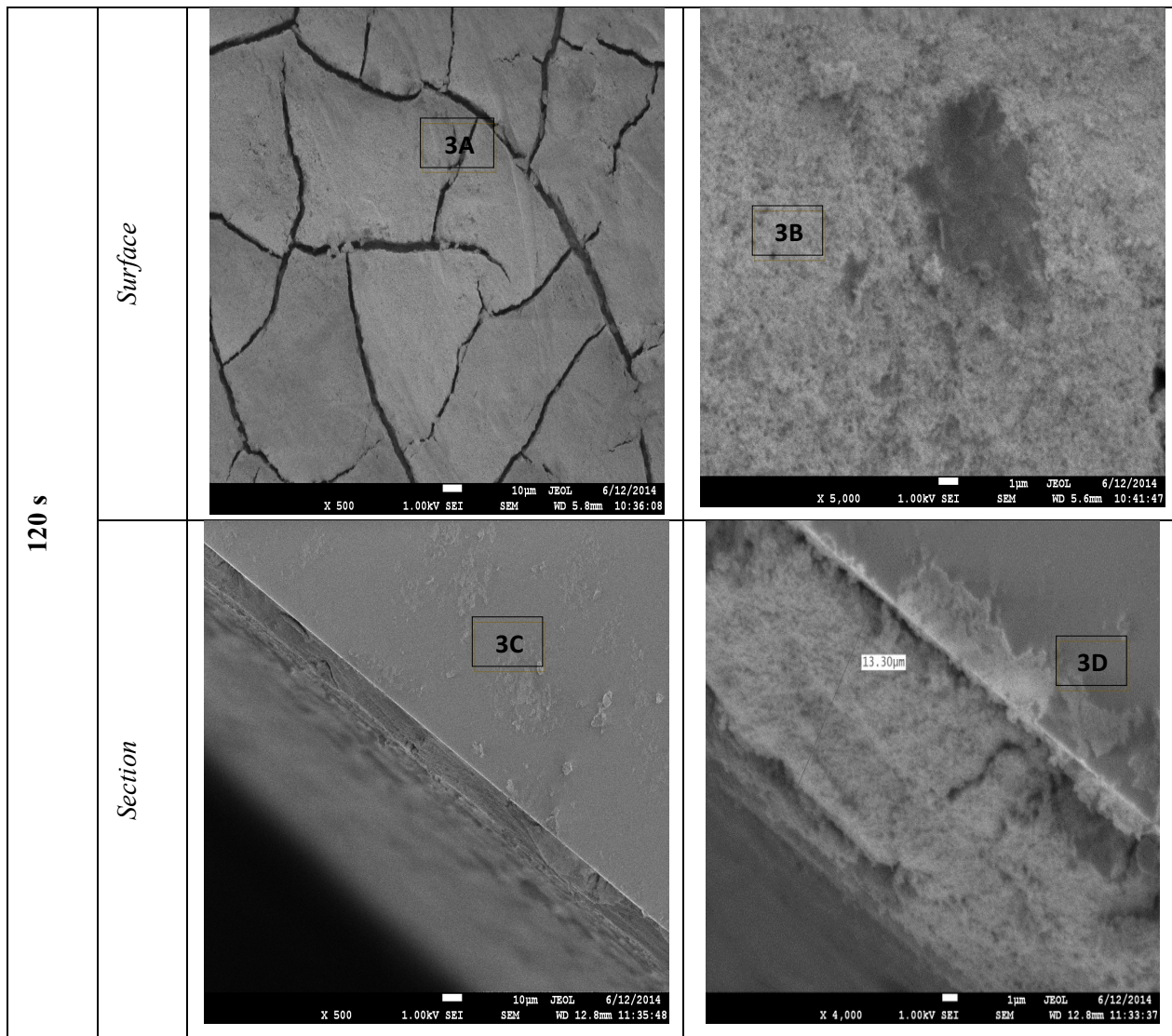


Figure 3. SEM image of thin film prepared on conducting glass during 120s at different magnifications

3.2. Influence of substrate and deposition time on photocatalyst amount

The evolution of photocatalyst masses deposited with time ranging from 40 s to 80 s (**Fig. 4**) shows that, whatever the substrate, photocatalyst amount is proportional to deposition time. However, when deposition time increases to 120 s, a deviation from linearity is noted only for stainless steel. Indeed, when deposition time increases, the number of TiO₂ particles mobilized toward the cathode increases leading to an increase in the mass deposited (kg) according to Hamaker's law [27,29]:

μ : Electrophoretic mobility ($\text{m}^2 \cdot \text{V}^{-1} \cdot \text{s}^{-1}$)

E : Strength of electric field ($\text{V} \cdot \text{m}^{-1}$)

A : Surface of electrodes (m^2)

C : Mass concentration of catalyst ($\text{kg} \cdot \text{m}^{-3}$)

t : Deposition time (s)

$$m = \mu \times E \times A \times C \times t \quad \text{Equation 4}$$

The parameters influencing electrophoretic deposition are based either on sol gel suspension or the process itself (applied voltage, electrode surface etc.) [30]. Whatever the time, the concentration of the suspension used can be considered constant ($12.5 \text{ g} \cdot \text{L}^{-1}$) during the deposition. It appears that the deviation from linearity would be attributable to the process.

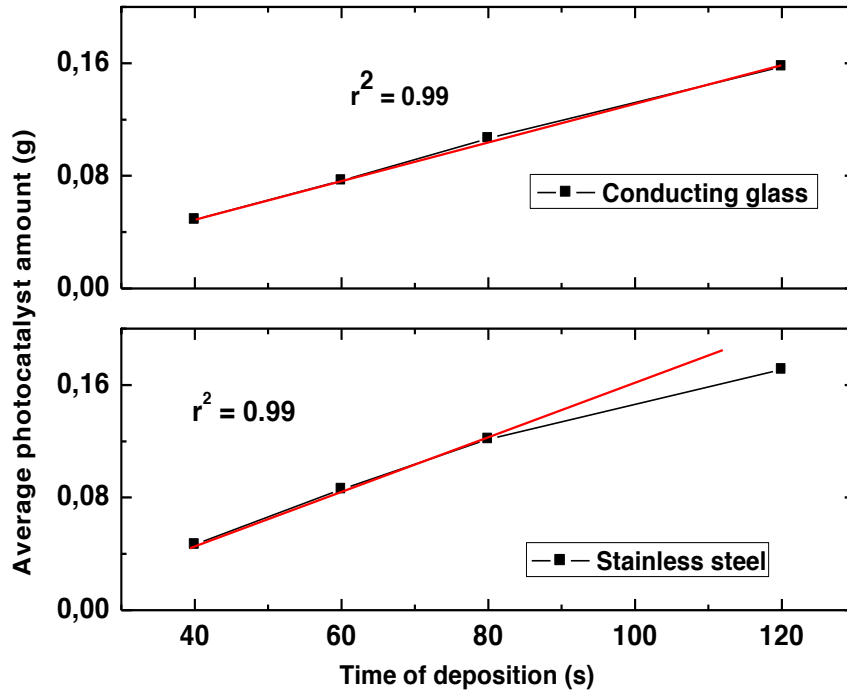


Figure 4. Evolution of TiO₂ amount deposited on stainless steel and conducting glass recorded with deposition time

Some authors have shown that when deposition time increases, deposition rate can decrease [31] to a constant value with very high deposition time. *Besra et al.*[30] reported further that when deposition time increases even with a constant applied voltage between the electrodes, the electric field decreases due to the formation of an insulating layer formed of the particles at the electrode surface. The deposited mass acts as a screen with a much higher electrical resistance than that of the suspension from which the deposit is made. Thus, when the deposition time increases, electrical driving force available decreases after some time leading to decrease of the deposition velocity. Also, according to *Ithurbide et al.*[21], the thickness can also become constant after some time for the same reasons as those mentioned above. It appears therefore that the factors influencing the electrophoretic deposit are dominantly those relating to the process. The deviation from linearity observed (**Fig. 4**) is significant with the stainless steel substrate probably because of the difference in resistance of the two conductive surfaces. Indeed, according to Ohm's law, the voltage applied between two electrodes is proportional to the current passing through the two electrodes, with resistance as coefficient of proportionality. Also according to review on kinetics of electrophoretic deposition stated by *Van der Biest et al.* [32] (**Equation 5**), the potential drop at electrodes, resistances of suspension and deposit could affect the value of electric field (E ; **Equation 6**) in the suspension and then mass of deposit.

$$V = \Delta\phi_1 + I \times R_d d_1 + I \times R_s (d - d_1) + \Delta\phi_2 \quad \text{Equation 5}$$

$\Delta\phi_i$: Potential drop at electrode i (V)

R_d : Resistance of deposit per unit length (Ohm.m⁻¹)

R_s : Resistance of suspension per unit length (Ohm.m⁻¹)

I : Current (A)

V : Applied potential (V)

d : Inter - electrode distance

d_1 : Thickness of deposit

$$E = \frac{V}{d} \quad \text{Equation 6}$$

In addition to prior factors presented and according to experimental conditions, the potential drop at electrodes influences mass of deposit concerning the nature of substrates.

3.3. Photocatalytic degradation of phenol in aqueous media: effect of deposit mass and substrates

Phenol degradation kinetic during 180 min was used to compare photocatalytic activity of films prepared by electrophoretic deposition using deposit times of 40, 60, 80 and 120 s on stainless steel and conducting glass.

Our previous work [25] showed that, using the same deposition condition, the photoactivity of the same photocatalyst on conducting glass is slightly higher than that obtained on stainless steel.

Figure 5 shows the phenol degradation kinetic recorded during 180 minutes. Regarding each support, there is no significant difference in phenol degradation percentage comparing the four thin layers obtained with deposition times of 40 to 120 s.

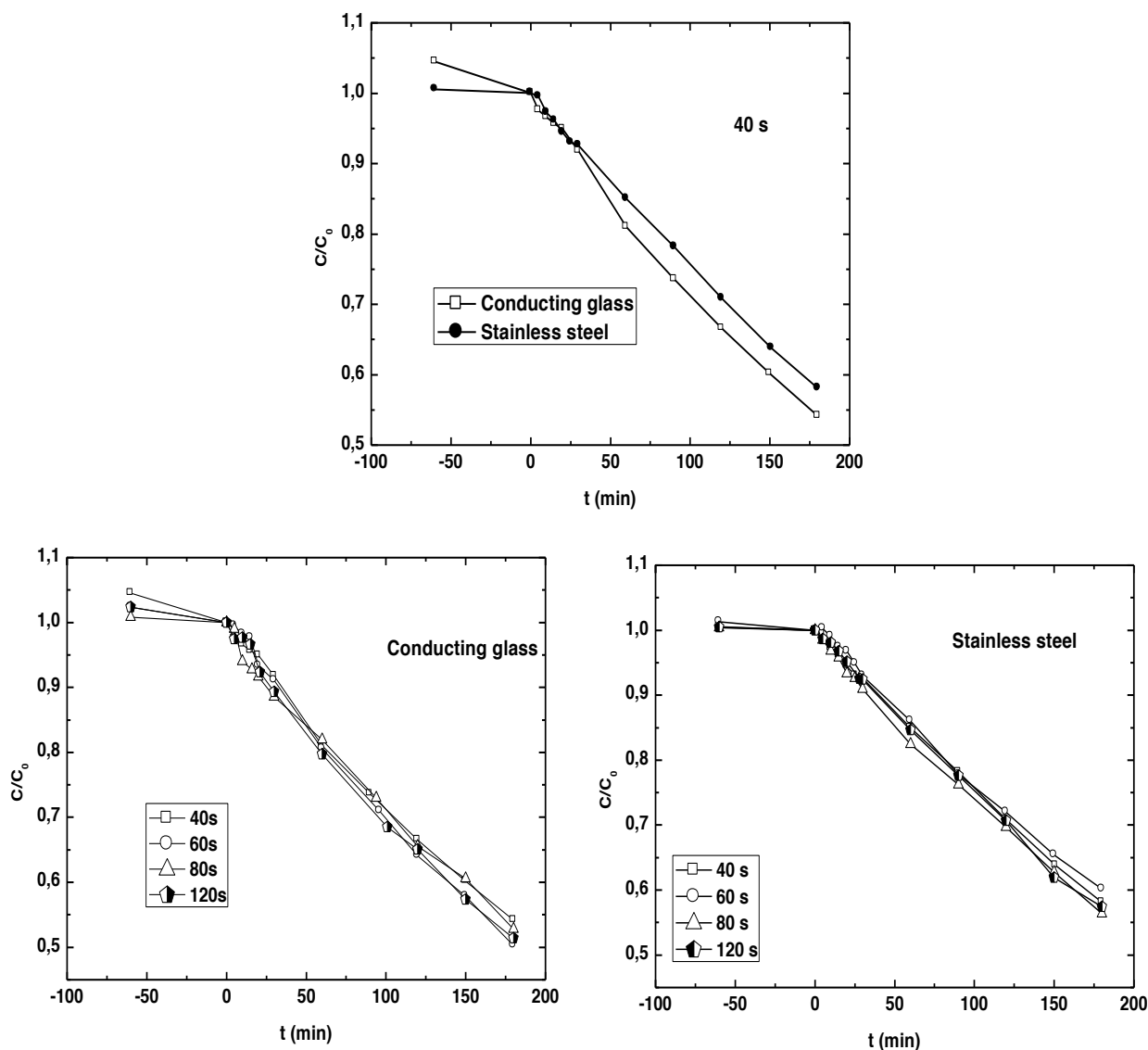


Figure 5. Effect of support and time used of $\text{TiO}_2\text{P25}$ deposition by EPD during phenol removal ($C = 100 \mu\text{mol.L}^{-1}$, free pH).

Under our experimental conditions, catalytic activity is not a function of mass of catalyst. It seems that from a certain mass of catalyst deposited, phenol removal is no longer a function of surface concentration. However, with regard to the influence of substrate, the photodegradation rates obtained with the catalysts on conductive glass are greater than those obtained on stainless steel.

The photocatalytic activity of deposits in terms of mineralization is however different comparing stainless steel and conducting glass used as support (**Table 1**). The phenol mineralization percentage was always greater on conducting glass. The result showed also that, mineralization varies little with the deposited mass of catalyst in

the case of conducting glass whereas it varies significantly with thin films prepared on stainless steel. Mineralization obtained decreases with increasing deposition time.

In terms of interdiffusion phenomena, some authors reported that temperatures, even low, could induce with FTO, diffusion of matter, especially tin (Sn) in the TiO₂. Above temperature of 500°C, sintering could be detrimental to photocatalytic activity[33]. Moreover Sn-doped rutile TiO₂ can effectively slow down the recombination rate due to band gap elevation of rutile TiO₂ and enhance photocatalytic activity[27].

Other authors have also reported a diffusion of Cr, Fe and Mn in the TiO₂ deposit when the stainless steel is calcined. The main forms of these metals are respectively Cr³⁺, Fe³⁺, Mn³⁺. This species can act as recombination center which is well-known to be detrimental to photocatalytic oxidation. However, the diffusive amount of these metals could be limited by the thickness of the deposit of TiO₂[34]. Then, if deposits made over a period of time greater than 40 s have the same photocatalytic activity, mineralization at least should be much greater if the diffusion is attenuated because of increasing of thickness. The results indicate a contrary trend meaning that others phenomenons act more on photocatalytic oxidation with this kind of substrates. The mineralization is similar on the other hand with the deposit made on the conductive glass. Therefore, interdiffusion in the bulk of deposit should be added to phenomenon as deposit saturation, porosity of film on stainless steel, in the conditions of preparation of the catalysts.

The photoactivity of TiO₂P25 is influenced by the type of substrate since the rate of abatement and mineralization of phenol evolves differently. Some authors have reported the role of porosity and light absorption capacity on photocatalytic activity. In the case of photocatalyst deposition, electrophoretic deposition is simultaneously accompanied with water electrolysis generating hydrogen (H₂) due to high voltage application [35]. In our study, the applied potential (10 V) to electrodes is not so high to induce water electrolysis. However, for the longest time, saturation of deposits in the case of stainless steel could promote this reaction. Therefore current hydrogen produced could induce an increase in the porosity of the thin layer. According to *Bandy et al.*[18], photocatalyst light absorption decreases when porosity becomes high. In addition the transmission of light on the film is increased up to a limit value where transmission is constant [36]. Therefore the photoactivity of TiO₂ will be similar regardless of the deposited mass. This phenomenon, would explain the similar kinetic abatement for phenol for films obtained with the 40 s deposition time. The decrease in mineralization obtained with thin films prepared on stainless steel when deposition time increases may be due to increasing porosity of layers leading to a decrease of light absorption. This porosity could induce also, in spite of thickness as reported by *Chen et al.*[34], a diffusion of metal ions from stainless steel substrates towards film.

Table 1. Percentage of phenol mineralization during photocatalytic test - effect of photocatalyst support and time used to prepare thin film

Deposition time during EPD(s)	40	60	80	120
Mineralization (%) in 3h after photocatalysis with stainless steel as catalyst support	21	12	10	10
Mineralization (%) in 3h after photocatalysis with conducting glass as catalyst support	30	28	31	33

4. Conclusion

The photoactivity of thin layer of TiO₂P25 electrodeposited on conducting glass and stainless steel with different deposition times was investigated. It appears that the photocatalytic activity of the deposited TiO₂P25 by EPD method depends on the support regarding phenol photooxidation and its mineralization. Increasing the amount of photocatalyst by increasing the time of deposition does not significantly affect photoactivity. However, phenol mineralization decreases significantly when deposition time varies from 40 to 120 s in the case of stainless steel as support. Phenol mineralization remains similar in the case of conducting glass as support. For application in water treatment, it is important to find the optimal condition of thin layer preparation. Further researches will be done to assess the influence of inorganic oxidants on photocatalytic activities of films.

Acknowledgement-The authors thank “International Foundation for Science (IFS)”, and Organisation for the Prohibition of Chemical Weapons (OPCW) for their financial support through the Grant No. W/5417-1. The authors also wish to thank the Embassy of France for their financial support.

References

1. D. Friedmann, C. Mendive, D. Bahnemann, TiO₂ for water treatment: Parameters affecting the kinetics and mechanisms of photocatalysis. *Appl. Catal., B* 99 (2010) 398-406.
2. C.-H. Chiou, C.-Y. Wu, R.-S. Juang, Influence of operating parameters on photocatalytic degradation of phenol in UV/TiO₂ process. *Chem. Eng. J.* 139 (2008) 322-329.
3. H. Hamdi, A. Namane, D. Hank, A. Hellal, Coupling of Photocatalysis and Biological Treatment for Phenol Degradation: Application of Factorial Design Methodology. *JMES* 8(2017) 3953-3961.
4. F. Thevenet, O. Guaitella, J.-M. Herrmann, A. Rousseau, C. Guillard, Photocatalytic degradation of acetylene over various titanium dioxide-based photocatalysts. *Appl. Catal., B* 61 (2005) 58-68.
5. Y. Chen, D. D. Dionysiou, A comparative study on physicochemical properties and photocatalytic behavior of macroporous TiO₂-P25 composite films and macroporous TiO₂ films coated on stainless steel substrate. *Appl. Catal., A* 317 (2007) 129-137.
6. S. Alahiane, S. Qourzal, M. El Ouardi, M. Belmouden, A. Assabbane, Y. Ait-ichou, Adsorption et photodégradation du colorant indigo carmine en milieu aqueux en présence de TiO₂/UV/O₂. *J. Mater. Environ. Sci.* 4(2013) 239-250.
7. F. Collignon, Cahier technologique sol gel. *Centre de Ressource Technologique en Chimie/ www.certech.be*, 2008; p 142.
9. G. Balasubramanian, D. D. Dionysiou, M. T. Suidan, I. Baudin, J.-M. Lainé, Evaluating the activities of immobilized TiO₂ powder films for the photocatalytic degradation of organic contaminants in water. *Appl. Catal., B* 47 (2004) 73-84.
10. D. Dumitriu, A. R. Bally, C. Ballif, P. Hones, P. E. Schmid, R. Sanjinés, F. Lévy, V. I. Pârvulescu, Photocatalytic degradation of phenol by TiO₂ thin films prepared by sputtering. *Appl. Catal., B* 25(2000) 83-92.
11. I. Burlacov, J. Jirkovský, M. Müller, R. B. Heimann, Induction plasma-sprayed photocatalytically active titania coatings and their characterisation by micro-Raman spectroscopy. *Surf. Coat. Technol.* 201 (2006) 255-264.
12. H. Lee, M. Y. Song, J. Jurng, Y.-K. Park, The synthesis and coating process of TiO₂ nanoparticles using CVD process. *Powder Technol.* 214(2011) 64-68.
13. H. M. Yates, M. G. Nolan, D. W. Sheel, M. E. Pemble, The role of nitrogen doping on the development of visible light-induced photocatalytic activity in thin TiO₂ films grown on glass by chemical vapour deposition. *J. Photochem. Photobiol., A* 179(2006) 213-223.
14. E. Lugscheider, G. Krämer, C. Barimani, H. Zimmermann, PVD coatings on aluminium substrates. *Surf. Coat. Technol.* 74(1995) 497-502.
15. K.-W. Weng, Y.-P. Huang, Preparation of TiO₂ thin films on glass surfaces with self-cleaning characteristics for solar concentrators. *Surf. Coat. Technol.* 231(2013) 201-204.
16. C. Guillard, D. Debayle, A. Gagnaire, H. Jaffrezic, J.-M. Herrmann, Physical properties and photocatalytic efficiencies of TiO₂ films prepared by PECVD and sol-gel methods. *Mater. Res. Bull.* 39(2004) 1445-1458.
17. C. Sarantopoulos. Photocatalyseurs à base de TiO₂ préparés par infiltration chimique en phase vapeur (CVI) sur supports microfibreux. *Doctorate thesis, INP Toulouse*, (2007) p180.
18. D. Matthews, A. Kay, M. Gratzel, Electrophoretically deposited titanium dioxide thin films for photovoltaic cells. *Aust. J. Chem.* 47(1994) 1869-1877.
19. J. Bandy, Q. Zhang, G. Cao, Electrophoretic Deposition of Titanium Oxide Nanoparticle Films for Dye-Sensitized Solar Cell Applications. *Mater. Sci. Appl.* 2(2011) 1427-1431.
20. M. M. Mohammadi, M. Vossoughi, M. Feilizadeh, D. Rashtchian, S. Moradi, I. Alemzadeh, Effects of electrophoretic deposition parameters on the photocatalytic activity of TiO₂ films: Optimization by response surface methodology. *Colloids Surf., A* 452(2014) 1-8.
21. X. Cui, Z. Yu, M. Ma, P. K. Chu, Nanocrystalline titanium nitride films prepared by electrophoretic deposition. *Surf. Coat. Technol.* 204(2009) 418-422.

22. J. G. Ibanez, M. Hernandez-Esparza, C. Doria-Serrano, A. Fregoso-Infante, M. M. Singh, The Point of Zero Charge of Oxides. *In Environmental Chemistry: Microscale Laboratory Experiments*, Springer New York: New York, NY, 2008; pp 70-78.
23. T. Kodom, E. Amouzou, G. Djaneye-Boundjou, L. M. Bawa, Photocatalytic discoloration of methyl orange and indigo carmine on TiO₂ (P25) deposited on conducted substrates: effet of H₂O₂ and S₂O₈²⁻. *Int. J. Chem. Technol.* 4(2012) 45-56.
24. S. C. Dixon, D. O. Scanlon, C. J. Carmalt, I. P. Parkin, n-Type doped transparent conducting binary oxides: an overview. *J. Mater. Chem. C* 4(2016) 6946-6961.
25. J. F. Porter, Y.-G. Liz, C. K. Chan, The effect of calcination on the microstructural characteristics and photoreactivity of Degussa P-25 TiO₂. *J. Mater. Sci.* 34 (1999) 1523 – 1531.
26. A. A. Dougna, B. Gombert, T. Kodom, G. Djaneye-Boundjou, S. O. B. Boukari, N. K. V. Leitner, L. M. Bawa, Photocatalytic removal of phenol using titanium dioxide deposited on different substrates: Effect of inorganic oxidants. *J. Photochem. Photobiol.*, A305(2015) 67-77.
27. J. M. Herrmann, Heterogeneous photocatalysis: state of the art and present applications. *Top.Catal.* 34(2005) 49-65.
28. Jun Lin, Jimmy C. Yu, D. Lo, S. K. Lam, Photocatalytic Activity of Rutile Ti_{1-x}Sn_xO₂ Solid Solutions. *J. Catal.* 183(1999) 368–372.
29. C. Audigié, G. Dupont, F. Zonszain, Principes des méthodes d'analyse biochimique. *Doin*(1992) 174.
30. H. C. Hamaker, Formation of a deposit by electrophoresis. *Trans. Faraday Soc.* 35(1940) 279-287.
31. Masao Kaneko, Ichiro Okura, *Photocatalysis : science and technology*. Japon, 2002.
32. A. M. Roy, G. C. De, N. Sasmal, S. S. Bhattacharyya, Determination of the flatband potential of semiconductor particles in suspension by photovoltage measurement. *Int. J. Hydrogen Energy* 20(1995) 627-630.
33. O. O. Van der Biest, L. J. Vandeperre, Electrophoretic deposition of materials. *Annu. Rev. Mater. Sci.* 29(1999) 327-352.
34. Codrin Andrei, Dominic Zerulla, Optimisation of Ruthenium Dye Sensitised Solar Cells Efficiency via Sn Diffusion into the TiO₂ Mesoporous Layer. *PLoS One* 8(2013) e63923.
35. Y. Chen, D. D. Dionysiou, TiO₂ photocatalytic films on stainless steel: The role of Degussa P-25 in modified sol-gel methods. *Appl. Catal., B* 62(2006) 255-264.
36. J. Senthilnathan, L. Philip, Photocatalytic degradation of lindane under UV and visible light using N-doped TiO₂. *Chem. Eng. J.* 161(2010) 83-92.
37. W. Wang, Y. Ku, The light transmission and distribution in an optical fiber coated with TiO₂ particles. *Chemosphere* 50(2003) 999-1006.

(2017) ; <http://www.jmaterenvirosci.com>